UNCLASSIFIED
UNLIMITED DISTRIBUTION

DREV REPORT 4310/83
FILE: 3633H-007
OCTOBER 1983

CRDV RAPPORT 4310/83
DOSSIER: 3633H-007
OCTOBRE 1983

CHEMICAL GENERATION AND DEACTIVATION OF OXYGEN SINGLET DELTA

S.A. Barton

Centre de Recherches pour la Défense
Defence Research Establishment
Valcartier, Québec

BUREAU - RECHERCHE ET DEVELOPPEMENT
MINISTERE DE LA DÉFENSE NATIONALE
CANADA

RESEARCH AND DEVELOPMENT BRANCH
DEPARTMENT OF NATIONAL DEFENCE
CANADA

UNCLASSIFIED
UNLIMITED DISTRIBUTION

CHEMICAL GENERATION AND DEACTIVATION OF OXYGEN SINGLET DELTA

by

S. A. Barton

CENTRE DE RECHERCHES POUR LA DÉFENSE
DEFENCE RESEARCH ESTABLISHMENT
VALCARTIER
Tel: (418) 844-4271

Québec, Canada October/octobre 1983

ABSTRACT

The construction and operation of a chemical generator of $O_2(a^1\Delta g)$ are described. This system could be readily modified to drive a purely chemical iodine laser operating at 1.315 μm.

Optical techniques were developed for estimating the excited oxygen concentration that arrives at a downstream cavity at total O_2 pressures from 1 to 6 torr.

Mechanisms that explain the deactivation of excited O_2 in the gas stream are discussed. A value for the singlet delta energy-pooling rate constant is determined from the measured $O_2(a^1\Delta g)$ concentrations.

RÉSUMÉ

On décrit la construction et le fonctionnement d'un générateur chimique d'oxygène $O_2(a^1\Delta g)$. Ce système pourrait être facilement modifié afin d'actionner un laser à iode entièrement chimique qui fonctionne à 1.315 μm.

On a développé des techniques optiques afin d'estimer la concentration de l'oxygène excité qui arrive dans une cavité située en aval du générateur. Des pressions totales d'oxygène de 1 à 6 torrs ont été étudiées.

On discute des mécanismes qui expliquent la désactivation de l'oxygène excité dans le flot de gaz. À partir des concentrations mesurées de $O_2(a^1\Delta g)$, on détermine une constante de vitesse de désactivation par un processus appelé mise en commun de l'énergie (energy-pooling).

TABLE OF CONTENTS

1.0 INTRODUCTION

The three lowest bound electronic states of oxygen are denoted, in order of increasing energy, $O_2(X^3\Sigma_g^-)$, $O_2(a^1\Delta g)$ and $O_2(b^1\Sigma_g^+)$. For brevity these will be referred to as $O_2(X)$, $O_2(a)$ and $O_2(b)$ respectively throughout this report.

The first excited state, often called singlet delta oxygen, may be generated in a microwave discharge of pure oxygen, or by bubbling chlorine gas through an aqueous solution of basic hydrogen peroxide (for a review see Ref. 1). In 1978 it was first demonstrated (Ref. 2) that such chemically generated $O_2(a)$ can provide the energy required to sustain iodine atom lasing at 1315 nm. The potential of this purely chemical oxygen iodine laser (COIL) as a highly efficient, high-power source of directed energy has led to several reports of improvements in both the oxygen generator and laser output levels (Refs. 3-7), and to an assessment of its capability to drive the nuclear fusion process (Refs. 8, 9).

The fundamental process in the COIL is an exchange of electronic energy (E-E transfer) during collisions between $O_2(a)$ and ground state iodine $I(^2P_{3/2})$, producing $O_2(X)$ and excited $I(^2P_{1/2})$. This E-E transfer is fast (Ref. 10) because there is a near resonance between the participating electronic levels of the two species, and it is this speed that makes the population inversion in iodine possible. Proportions of $O_2(a)$ in excess of about 20% of the total oxygen are required to operate the iodine laser above threshold, and water vapour must be minimized as it is an efficient quencher. This threshold minimum precludes the use of the microwave discharge as an $O_2(a)$ generator in the I laser, since proportions of only 5-15% are attainable.

High energy storage densities are possible in $O_2(a)$. Firstly, because the chemical generation method is remarkably efficient, both in terms of reactant conversion and product purity, it gives close to

100% $O_2(a)$ at the generator. Secondly, the gas can be efficiently transported from generator to laser cavity in a vacuum flow system. $O_2(a)$ has a very long radiative lifetime (Ref. 11), and is not rapidly quenched by itself (energy-pooling), water vapour, or inert carrier gases (e.g. argon).

Downstream $O_2(a)$ percentages have been reported (Refs. 3-8) in the 25-60% range at pressures in the region of 1 torr total oxygen. The proportion of $O_2(a)$ arriving at a measurement cavity depends on several physical factors, principally: the pumping speed, i.e. the transport time from the generator; the total O_2 pressure; the condition and material of the walls; the temperature of any trap which may be installed to remove H_2O vapour; and the presence of other gases in the system.

Work was initiated at DREV to develop locally the technology for the chemical generation of $O_2(a)$ in order to provide a) the capability of building an iodine laser should the need arise, and b) an energy transfer medium for other potential gas laser systems. In particular we studied the energy transfer to gaseous nitrogen fluoride. The electronically excited NF so produced emits at 529 nm. This application of the chemical $O_2(a)$ generator to a potential blue-green laser gain medium will be the subject of future reports.

This report describes the operation of a prototype chemical generator of oxygen singlet delta (Chapter 2.0), and the measurement of $O_2(a)$ concentration at a downstream cavity (Chapter 3.0) by optical methods. In Chapter 4.0 the deactivation processes are discussed, and a value for the energy-pooling rate constant of $O_2(a)$ is calculated from the experimental data of Chapter 3.0. The energy pooling rate is important in modelling the maximum energy storage capability of singlet

delta oxygen. Its value influences chemical oxygen iodine laser output and efficiency predictions, and hence also the conclusions concerning its candidacy as a fusion driver.

This work was performed at DREV between January 1981 and October 1982 under PCN 33H07, Research on Chemically Excited Lasers.

2.0 CHEMICAL GENERATION

This chapter describes the construction and operation of a chemical generator of $O_2(a)$ similar to those described in Refs. 4 and 5.

The excited oxygen is generated by bubbling chlorine gas into an alkaline aqueous solution of hydrogen peroxide. The overall reaction is:

$$Cl_2 + 2OH^- + H_2O_2 = 2Cl^- + 2H_2O + O_2(a) \qquad [1]$$

The mechanism of this solution reaction is discussed in the literature (Refs. 6, 12, 13), and will not be considered here. It is sufficient to know that it is a very fast, essentially stoichiometric conversion, and that virtually no chlorine leaves the solution under the flow conditions quoted here.

2.1 Apparatus and Operation

Figure 1 is a schematic representation of the flow system which we have used to generate $O_2(a)$.

Vessels C to F and H were of Pyrex, as was the tubing between D and G. Where possible, tubing was of large diameter (40 mm) to minimize $O_2(a)$ losses by wall collision. The measurement cavity G was of rectangular cross section (1 x 12 cm), and about 30 cm long. It was

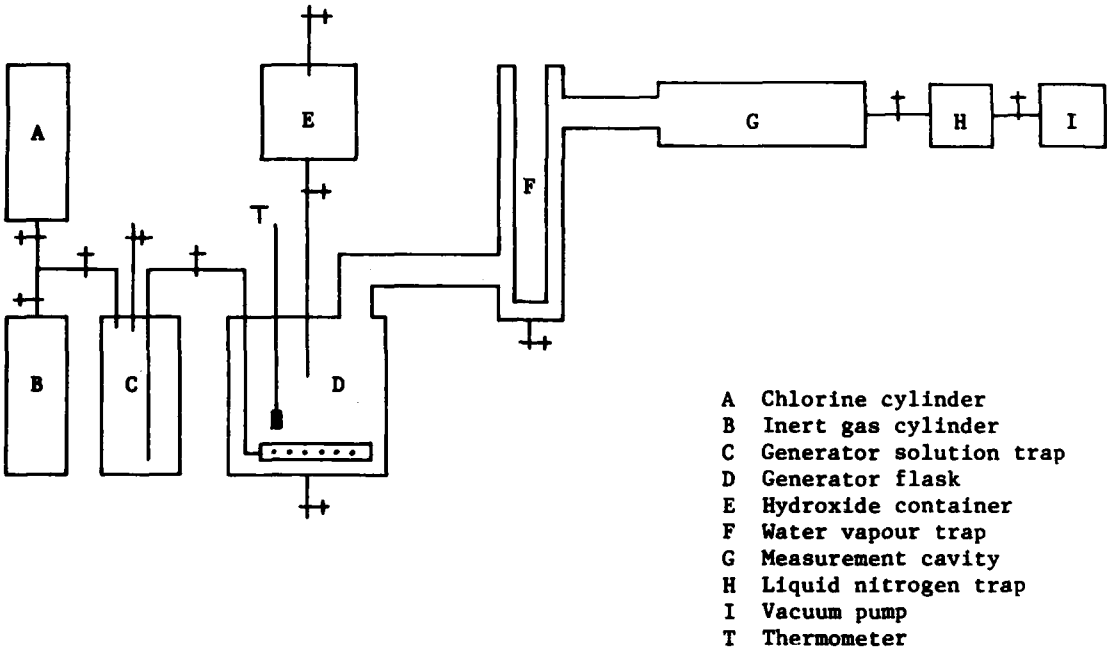

FIGURE 1 - Flow system for generation of oxygen singlet delta

made of Perspex coated on the inside with Teflon. Plastic was used, and the cavity was fitted with aluminum electrodes, so that high voltage discharges could be applied transverse to gas flows containing $O_2(a)$, nitrogen fluorides, and other gases. Gas flow rates and pressures were measured with calibrated Hastings flowmeters and capacitance manometers (MKS Baratron, Vacuum General) respectively. The vacuum pump was an Edwards 660, which is specified as being capable of displacing 11 L/s.

A brief description of the normal operating procedure for this system follows.

Initially, hydrogen peroxide (2 L of 30% by weight aqueous solution) is poured into the generator flask D (12 L spherical) with the system open to the atmosphere. This solution is then evaporatively cooled to about 15°C by evacuating the system to 10-15 torr. Vapour is solidified in the liquid nitrogen trap H before the vacuum pump I. A sodium hydroxide solution (500 mL, 40% by weight) is slowly allowed to enter the generator from the storage vessel E (1 L sphere) while a minimal flow (100 SCCM) of inert gas (argon) from B enters the solution through a bubbler. This bubbler was a 20 cm length of flexible plastic (Tygon) tubing, sealed at one end and pierced by about 100 holes of approximately 0.5 mm diameter. Trap C prevents liquid from flowing back into the gas handling system. Argon flow during the hydroxide addition ensures good mixing. This mixing is exothermic, and the solution temperature should be maintained below 20°C (to minimize H_2O_2 decomposition) by keeping the pressure below 15 torr. Under these conditions the mixing process takes about 20 min.

$O_2(a)$ is generated by flowing chlorine through the alkaline peroxide solution. The reaction (eq. 1) is exothermic. As the solution temperature increases so does the amount of ice collected in the liquid nitrogen trap. The water vapour pressure can, however, be maintained in the 1-2 torr range if, before starting the $C\ell_2$ flow, the solution is cooled to about -15°C by fully opening the system to the vacuum pump for about 30 min. Coolant may also be placed in trap F of Fig. 1 if it is important to minimize H_2O vapour at the measurement cavity.

This system, operating with chlorine flow rates up to 4000 SCCM, produces total pressures up to about 10 torr, of which (at -10°C) approximately 1 torr is water vapour. The generator can operate continuously for about 40 min at 1000 SCCM $C\ell_2$ and a total pressure of about 3 torr. After that, the solution hydroxide ion concentration and $O_2(a)$ production simultaneously fall rapidly, and $C\ell_2$ begins to pass through the generator.

2.2 Problems and Hazards

The hazards of working with $C\ell_2$ are well known (Refs. 14, 15). The very low recommended working threshold concentration of 1 ppm is below the minimum (3.5 ppm) normally detectable by its odour. Working areas must therefore be well ventilated, and precautions must be taken when disposing of the generally small quantities of chlorine that condense in the liquid nitrogen trap.

Highly concentrated hydrogen peroxide also presents serious safety hazards, which are well documented (Refs. 16, 17). At greater than 52% (by weight) H_2O_2, the rate at which heat is generated by decomposition may exceed that at which it is dissipated by evaporation of water from the solution. The explosive generation of large volumes of hot O_2/H_2O vapour can result. For this reason, 30% H_2O_2 has been used here rather than the 90% solution of the original chemical generators (Refs. 2-6).

Chloride ion is known to catalyse the decomposition of H_2O_2. The reaction sequence (given in Ref. 17, p. 476) is:

$$H_2O_2 + 2C\ell^- + 2H^+ = C\ell_2 + 2H_2O \qquad [2a]$$

$$H_2O_2 + C\ell_2 = 2C\ell^- + 2H^+ + O_2 \qquad [2b]$$

Therefore, at the end of an $O_2(a)$ generation experiment, the reactor solution is in an unstable condition since OH^- produces $C\ell^-$ in reaction 1. As the solution warms, the rate of the reaction sequence [2a]-[2b] increases, heat is evolved, and a violent decomposition ensues. This has occurred in our laboratory when the used reactor solution has been left overnight in the generator. It may be avoided by flushing away the still cool (< 20°C) solution with a large volume of cold water.

Removal of water vapour from the gas flow is a major problem. Even with solution temperatures in the -10°C to -15°C range, cold traps may become blocked with ice after 10-30 min of operation, depending on trap and solution temperatures and gas flow rates. At trap temperatures below about -70°C and gas temperatures below -35°C, there is also a significant deactivation of the excited oxygen (Ref. 6). A balance must be sought between permissible H_2O content and $O_2(a)$ deactivation.

Degradation of the vacuum pump oil must also be dealt with. The normal hydrocarbon-based pump oils are rapidly attacked by the activated oxygen (which is not condensed in liquid nitrogen at pressures in the 10 torr range), and also by traces of chlorine (most of which is solidified in the trap). These oils become viscous and dark brown after about one hour of continuous $O_2(a)$ generation. The risk of pump oil explosion cannot be ignored, particularly when other reactive gases (e.g. halogens, nitrogen fluorides) may be flowing during a laser experiment. Hydrocarbon oils should be replaced after each such experiment. Preferably, a completely inert pump fluid, such as Inland 41, should be used. For a pump of several litres capacity, this can be justified from considerations of both safety and economy, since this oil may remain unchanged during several months of continuous usage.

3.0 MEASUREMENT

Previously (Refs. 2-8, 18-22), electron paramagnetic resonance (EPR), isothermal calorimetry, and photometry have been used to estimate absolute concentrations of $O_2(a)$. Of these, EPR and photometry do not perturb the gas flow and are specific to the singlet delta state, whereas isothermal calorimetry requires the insertion of a probe into the flow and may be less specific if other excited species are present.

We chose to measure $O_2(a)$ using photon detection techniques for the above reasons, as well as because they can follow concentration changes in both space and time during a reaction with other species, and are inexpensive compared with the EPR method. The disadvantage is that accuracy may not be very high since it depends on uncertainties in detector calibration and a radiative rate constant.

$O_2(a)$ emits most strongly in two spectral regions: in the near infrared around 1268 nm, and in the visible centred at 634 nm (red). The former emission arises from direct spontaneous transitions between the vibrational ground states of the a and X electronic states (the 0-0 band of the $a^1\Delta g - X^3\Sigma\bar{g}$ system). Under low resolution, this band has a roughly Gaussian distribution with a full width at half maximum (FWHM) of about 15 nm (Ref. 23). At higher resolution the rotational fine structure has been partially resolved (Ref. 24). The red emission results from a collisional process involving two $O_2(a)$ molecules (hence the common name 'dimole' emission) that simultaneously transfer their electronic energy to one emitted photon. This dimole emission wavelength is thus half that of the direct a-X emission. The dimole band is diffuse with no resolved fine structure (Refs. 24-26) and an FWHM of 15 nm.

These two emission processes will be represented by:

$$O_2(a,0) \xrightarrow{k_s} O_2(X,0) + h\nu(1268) \qquad [3]$$

$$2O_2(a,0) \xrightarrow{k_d} 2O_2(X,0) + h\nu(634) \qquad [4]$$

The second bracketed index indicates the vibrational level ($v = 0$ in the cases indicated) within the electronic states a and X. The a-state $v' = 1$ level is insignificantly populated at room temperature (assuming a Boltzmann distribution), but transitions to the X-state $v'' = 1$ level do occur:

$$O_2(a,0) \rightarrow O_2(X,1) + h\nu(1580) \qquad [5]$$

$$2O_2(a,0) \rightarrow O_2(X,1) + O_2(X,0) + h\nu(703) \qquad [6]$$

The second dimole emission at 703 nm, indicated by [6], is of comparable intensity (Refs. 25, 27) to that at 634 nm, whereas the 1580 nm emission of [5] is 46 times lower in intensity than the 0-0 band (Ref. 23).

Radiative rate constants for processes [3] and [4] have been reported in the literature (Refs. 11, 28 and 18-20, 29 respectively). These constants directly relate the rate of emission of photons in the 1268 nm and 634 nm bands to $[O_2(a)]$ (the square brackets indicate concentration):

$$dh\nu(1268)/dt = k_s[O_2(a)] \qquad [7]$$

$$dh\nu(634)/dt = k_d[O_2(a)]^2 \qquad [8]$$

In [7] and [8] $dh\nu(\lambda_o)/dt$ is the number of photons emitted per second in the band centred at λ_o, from a volume of one cubic centimeter. Independent photometric methods based on these emissions can therefore be designed to estimate $[O_2(a)]$ without the need to consider other competing processes, such as [5] and [6], or the presence of other excited species ($O_2(b)$ for example).

We have observed both these emission bands with narrow-band interference filters and calibrated semiconductor detectors. The following sections (3.1 and 3.2) describe the apparatus used to produce voltage measurements from these detectors, and subsequent estimates of singlet delta concentrations in the O_2 generator gas flow.

3.1 Apparatus

The measurement cavity (G of Fig. 1) of the flow system was essentially a rectangular plastic box (described in Section 2.1) with planar Supracil II glass windows on the sides parallel to the gas flow. The viewing axis for the detectors and optics was thus perpendicular to the flow, and since the windows were sufficiently long, the field of view was unconstrained in the flow direction. A separate report (Ref. 30) presents a detailed development of the equations that describe the light collection from this particular extended source, for the two quite different optical arrangements that we have used experimentally. Namely, with (a) a circular focusing lens, and (b) a cylindrical tube placed between source and detector. The two arrangements provided independent methods for accurately defining the contributing volume of emitting molecules, and hence estimating their concentration.

Detectors were chosen for their high sensitivity in the two emission regions of interest: for the 634 nm band, an EG & G silicon HUV-4000B was used; for 1268 nm, it was a Judson Infrared germanium J-16. Appropriate narrow-band interference filters (the transmission characteristics of which are described in Appendix A) were placed directly in front of the detector surfaces, with care being taken to exclude all stray light. A chopper/lock-in amplifier combination was used to record accurately the voltage signals from these detectors. The detector/filter units were calibrated absolutely using both an NBS standardized quartz-iodine lamp, and two blackbody sources at 1000°C.

3.2 Results

Table I presents data from three experiments. For each experiment, column one shows a series of increasing total oxygen pressures (PO_2(total)) measured at the cavity G of Fig. 1. This total O_2 pressure was controlled by increasing the mass flow rate of $C\ell_2$ through the

generator, with the pump operating at its maximum capacity (all pump control valves fully open). The O_2 pressure was estimated by measuring the pressure in the system immediately before (giving $H_2O + H_2O_2$ vapour pressure) and after the $C\ell_2$ flow was started, and then again before and after the flow was stopped. The average of these pressure differences was taken to be a measure of PO_2 (total). This assumes that no $C\ell_2$ passed through the generator solution, which is supported by the fact that no significant $C\ell_2$ was collected in the liquid nitrogen trap (H of Fig. 1) at the flow rates used in these experiments. The estimated PO_2 (total) was quite linear with $C\ell_2$ mass flow: e.g. 750 SCCM $C\ell_2$ gave ~ 1 torr O_2, 1500 SCCM gave ~ 2 torr, etc.

Column two of Table I shows voltages recorded at the lock-in amplifier from the germanium and silicon detector/filter combinations for the different total oxygen pressures. For the lens and tube optical arrangements respectively, eqs. 81 and 82 of Ref. 30 relate the detector voltages from the spontaneous emission (1268 nm) to the oxygen singlet delta concentrations, thus:

(i) lens case (1268 nm - germanium),

$$[O_2(a)] = 4\pi\Gamma V/(wtf)(\ell tf)(ftf)k_s I_L \qquad [9]$$

(ii) tube case (1268 nm - germanium),

$$[O_2(a)] = 4\Gamma V/(wtf)(ftf)k_s I_T r^2 \qquad [10]$$

For the dimole emission (634 nm), the photon emission rate depends on the square of the $O_2(a)$ concentration (eq. 8), and thus [10] becomes:

(iii) tube case (634 nm - silicon),

TABLE I

Oxygen singlet delta concentrations from detector voltages

PO_2 (torr)	Voltage (Microvolts)	$[O_2(a)]$ (Molecules.cm^{-3})	$PO_2(a)$ (torr)	% $O_2(a)$
i) Germanium detector + lens:				
1.01	186	7.57 E15	0.230	22.8
2.08	340	1.38 E16	0.421	20.2
3.24	486	1.98 E16	0.601	18.6
4.00	516	2.10 E16	0.639	16.0
ii) Germanium detector + tube:				
1.16	11.5	8.28 E15	0.252	21.7
2.19	18.5	1.33 E16	0.405	18.5
3.26	25.5	1.84 E16	0.558	17.1
3.99	27.5	1.98 E16	0.602	15.1
iii) Silicon detector + tube:				
1.02	0.30	9.26 E15	0.281	27.6
2.03	0.88	1.59 E16	0.482	23.7
3.29	1.53	2.09 E16	0.636	19.3
4.44	1.95	2.36 E16	0.718	16.2
6.00	2.40	2.62 E16	0.796	13.3

$$[O_2(a)] = [4\Gamma V/(wtf)(\ell tf)(ftf)k_d I_T r^2]^{\frac{1}{2}} \qquad [11]$$

The terms in eqs. 9 to 11 are:

Γ - detector calibration constant (chopping frequency 23 Hz),
germanium (1268 nm filter) - 1.3E14 photons $s^{-1}v^{-1}$;
silicon (634 nm filter) - 9.8E12 photons $s^{-1}v^{-1}$;

V - detector voltage measured at lock-in amplifier (in volts);

wtf, ℓtf, ftf - window, lens, and filter transmission factors at the appropriate wavelength (see Appendix A);

k_s and k_d - spontaneous and dimole emission rate constants,
k_s = 2.6E-4 s^{-1} (Refs. 11, 28),
k_d = 4.1E-23 cm^3 $molecule^{-1}s^{-1}$ (an average of three reported values (Ref. 18));

I_L and I_T - integrals over the extended source volume for the lens and tube cases respectively (their calculation is described in detail in Ref. 30);

r - active detector radius.

Equations 9 to 11 lead to the values for $[O_2(a)]$ (molecules cm^{-3}) given in column 3 of Table I. The table also shows these values in torr (at 20°C, 1 torr = 3.29E16 molecules cm^{-3}) so that the percentage of $O_2(a)$ in the measured total oxygen can be readily estimated.

It can be seen that by increasing the total oxygen pressure (increasing the $C\ell_2$ flow) the absolute concentration of $O_2(a)$ arriving at the cavity can be increased, but that in doing this the percentage

of $O_2(a)$ in the stream is reduced. This is largely due to the energy-pooling process mentioned in Chapter 1.0:

$$2O_2(a) \xrightarrow{k_p} O_2(X) + O_2(b) \qquad [12]$$

The rate of this reaction will be discussed in Chapter 4.0

The absolute accuracy of the $O_2(a)$ concentrations can be estimated from eqs. 9 to 11. The detector calibrations (Γ) and extended source integrals (I_L, I_T) each have uncertainties of about 10%, while those for the voltages and transmission factors are on the order of 1-2%. The error in the radiative rate constants (k_s, k_d) is more difficult to estimate. The value of k_s given by Badger et al (Ref. 8), 2.6E-4 s^{-1}, is generally accepted in the literature, and agrees within 10% with other quoted values (Refs. 8, 28). The dimole emission rate constant k_d has been directly measured by four independent groups (Refs. 18-20, 29). Of these, three agree to within 10% (Ref. 18), whereas the value found by Derwent and Thrush (Ref. 20) is smaller by a factor of two.

An uncertainty of about 30% is therefore expected in the $[O_2(a)]$ values given in Table I from observation of the direct spontaneous emission (germanium detector).

The concentrations estimated from the dimole emission (silicon detector) have an inherently higher accuracy due to the square root relationship in [11]. The values from the silicon detector in Table I therefore have an uncertainty of about 15%.

Figure 2 shows the calculated partial pressures of $O_2(a)$ arriving at the measurement cavity for each of the measured total oxygen pressures in the two detector data sets.

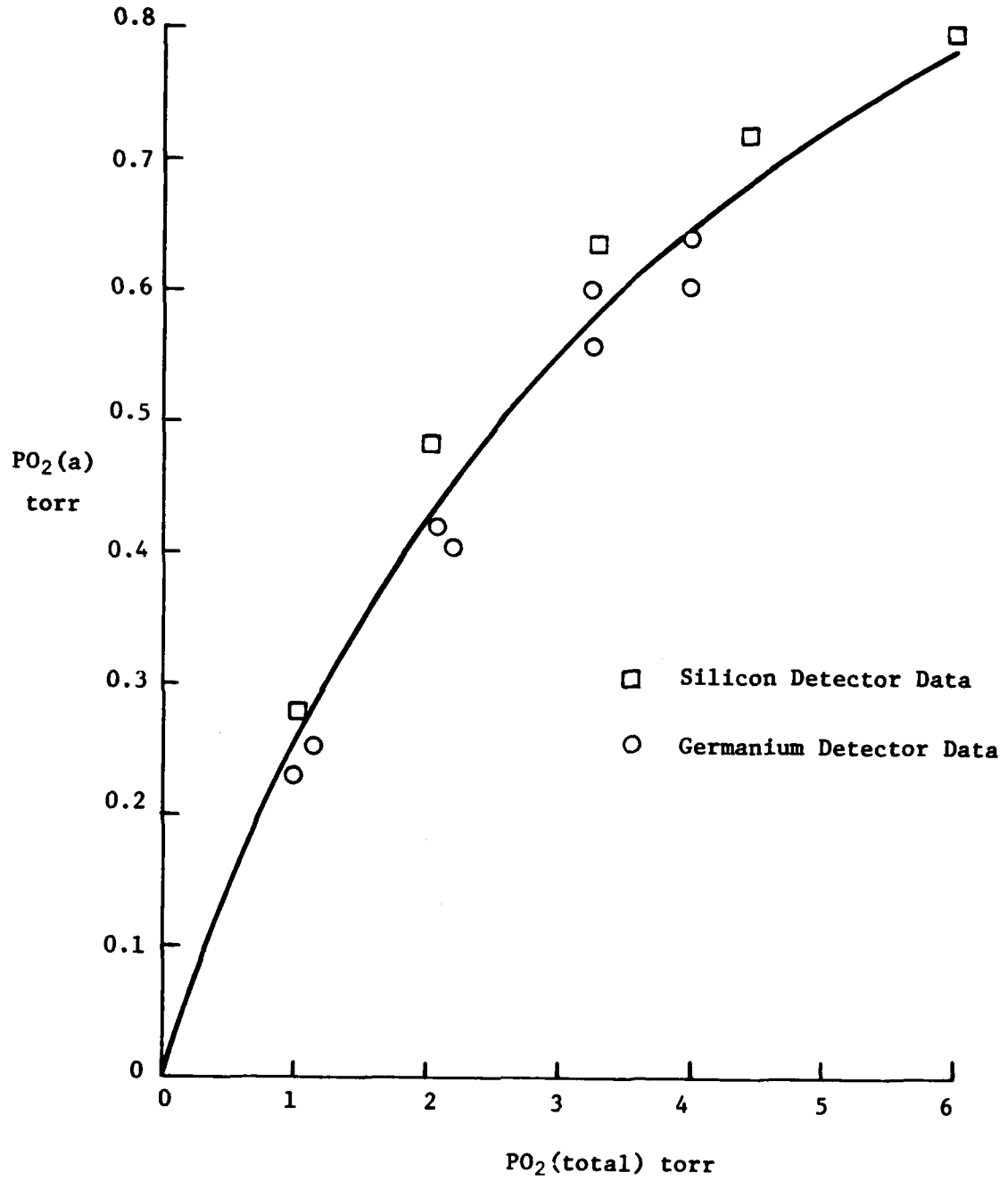

FIGURE 2 - PO_2(a) vs PO_2(total)

It is significant that the $[O_2(a)]$ values calculated from the germanium detector data were consistently lower than those calculated from the silicon detector voltages. The differences are somewhat greater than would be expected from uncertainties in the detector calibrations alone, and suggest that the accepted value for the spontaneous radiative rate constant (k_s = 2.6E-4 s^{-1}) for $O_2(a)$ may be rather high. The dimole emission rate constant has been more extensively studied and is probably more reliable.

The curve drawn through the experimental points has the functional form:

$$y(x) = x/(a + bx) \qquad [13]$$

($y \equiv PO_2(a)$; $x \equiv PO_2(total)$).

This form was chosen because it has the correct asymptotic behaviour ($y \to$ constant $(1/b)$ as $x \to \infty$) for a second-order-dominated decay process, and it leads to a better least-squares fit than the other simple two-parameter forms ax^b and $x(a + bx)$. Since there are eight data points from the germanium detector and only five from the silicon, a weighted fit was performed giving the silicon points 1.6 times the weight of the germanium points. This means that the data sets from each detector were treated equally.

The resulting values for the constants of [13] are:

$$a = 3.213 \quad ; \quad b = 0.7449 \qquad [14]$$

No physical significance is to be attached to these values. Equations 13 and 14 merely provide a continuous representation of the $O_2(a)$ partial pressure at the cavity as a function of total O_2 pressure.

3.3 Inert Gas Diluents

We have studied the effect on the $O_2(a)$ emissions of introducing up to 10 torr of either argon or sulphur hexafluoride into the gas stream. The diluent gas was premixed with the $C\ell_2$ and passed directly through the generator solution.

No detectable effect has been observed on either the 1268 nm or 634 nm emission intensities for any fixed $C\ell_2$ flow rate. These observations are in accord with the reported (Refs. 31, 32) low $O_2(a)$ quenching rate constants (1E-20 cm^3 $molecule^{-1}$ s^{-1}) for these gases. Inert behaviour can also be expected for nitrogen and helium on the basis of their similarly low quenching rates.

3.4 Water Vapour

At a generator solution temperature of -10°C there was about 1 torr of solution vapour in the flow system, measured at the cavity. This was essentially all water vapour since the mole fraction of H_2O_2 in the vapour above a 30% aqueous solution is < 0.003 (Ref. 17, page 227) at this temperature. As $C\ell_2$ flows into the reactor the solution temperature rises slowly (about 1°C per minute for 2000 SCCM of $C\ell_2$), and the measured emission intensity declines steadily as this temperature exceeds approximately 0°C.

The $O_2(a)$ quenching rate constant for H_2O is about 5E-18 cm^{-3} $molecule^{-1}$ s^{-1} (Refs. 31, 32), which is sufficiently high to produce a measurable effect with increasing H_2O vapour pressure (see Chapter 4.0). Operating the generator at a solution temperature between -10°C and -5°C (in the 1-2 torr H_2O pressure range) does not give a significant variation in emission intensity for a fixed $C\ell_2$ flow. The measurements given in Table I were all taken with the solution in this temperature range.

3.5 Vapour Removal by Liquid Nitrogen Trap

The effect of trap temperature on the percentage $O_2(a)$ in the flow has been studied extensively elsewhere (Refs. 6, 7). We used liquid nitrogen in trap F of Fig. 1 to study how almost entirely removing H_2O from the flow affects reactions with NF radicals. Under these conditions the percentage of $O_2(a)$ is dramatically reduced to between 3 and 5% for the pressure range 1-4 torr total O_2 (cf. 25-16% in Fig. 2 for these pressures). Trap temperatures as low as -78°C (acetone/dry ice) are possible (Ref. 7) without significant quenching of $O_2(a)$.

4.0 DEACTIVATION

First and second order rate constants quoted in this and subsequent sections have the units s^{-1} and cm^3 molecule^{-1} s^{-1} respectively. Concentrations are in molecules cm^{-3} unless otherwise stated.

There are three principal mechanisms for the deactivation of $O_2(a)$.

(i) Energy Pooling: $2A \xrightarrow{k_p} B + X$ [15]

(ii) Quenching: $A + Qi \xrightarrow{k^A_{Qi}} X + Qi$ [16]

(iii) Wall Collisions: $A \xrightarrow{k^A_w} X$ [17]

In [15]-[17] A, B and X represent $O_2(a)$, $O_2(b)$ and $O_2(X)$ respectively, and Qi is any other gaseous molecule that may be present (H_2O, Ar, and $O_2(x)$). The same alphabetic symbol will represent species concentration whenever there is no ambiguity.

Radiative losses (eqs. 3 to 6) are negligible in the time domain considered here (< 1s).

In this section, an equation determining the rate of change of $[O_2(a)]$ is developed, and the integrated form is derived. The $O_2(a)$ concentration is then defined for all time in terms of the initial gas concentrations and the reaction rate constants. The $[O_2(a)]$ curve of Fig. 2 can therefore be reproduced, given the flow time from generator to measurement cavity, using a particular set of rate constants.

The rate of loss of A due to reactions [15]-[17] is:

$$-A'(t) = 2k_p A^2 + (k_w^A + \sum_i k_{Qi}^A Qi)A \qquad [18]$$

Note that the sum over i includes all quenching species in the flow, and that the rate of loss of A due to pooling is written $2k_p A^2$ in agreement with the literature (Refs. 20, 21, 36, 37) definition of k_p (which is the rate constant for the formation of B and X).

There is a great deal of evidence in the literature (Refs. 37-44) to indicate that the $O_2(b)$ produced by the pooling reaction [15] is quenched to $O_2(a)$ both by other gaseous species, and wall collisions. Reactions that produce A must therefore be included:

$$B \xrightarrow{k_w^B} A \qquad [19]$$

$$B + Qi \xrightarrow{k_{Qi}^B} A + Qi \qquad [20]$$

Equations may now be written for the overall rate of change of the components A and B. Including [19] and [20] in [18] gives:

$$A'(t) = K_B B - 2k_p A^2 - K_A A \qquad [21]$$

where:

$$K_I = k_w^I + \sum_i k_{Qi}^I Qi \quad ; \ (I = A, B) \qquad [22]$$

The rate equation for B due to reactions [15], [19] and [20] is:

$$B'(t) = k_p A^2 - K_B B \qquad [23]$$

Water vapour is abundant in the chemical generation of $O_2(a)$, and it is an extremely rapid quencher of $O_2(b)$. Indeed, $k_{H_2O}^B$ is about 5E-12 (Refs. 31, 38, 45, 46), so that for 1.5 torr H_2O the pseudo-first order quenching rate is roughly 250,000 s^{-1}. Other quenchers, and wall collisions, are completely negligible in the term for K_B (eqs. 22 and 23): $k_{O_2}^B$ is, for example, approximately 4E-17 (Refs. 38, 47-49). $O_2(a)$, however, is quenched about a million times more slowly by water vapour than is $O_2(b)$ (Refs. 31, 32). This rapid B quenching appears to be due to a near resonance between the O_2 b-a energy spacing and a vibrational mode of H_2O.

The effect of this very fast conversion of B to A is that a quasi-steady-state for B is established very rapidly: for 1 torr of initial A, B rises to an essentially constant value in ~ 5E-5 s. This was calculated by exactly solving the coupled eqs. 21 and 23 with rate constants from the literature using the general chemical kinetics FORTRAN program described in Ref. 50. The quasi-steady-state concentration of B is obtained from [23]:

$$B(t) = k_p A^2 / K_B \qquad [24]$$

and subetitution of B in eq. 21 leads to a partially decoupled rate equation for A:

$$A'(t) = -k_p A^2 - K_A A \qquad [25]$$

A(t) is still coupled to X(t) through the term in K_A due to the quenching of A by X (cf. eq. 16). The case Qi = X will be separated from the general quenching summation:

$$-A'(t) = k_p A^2 + (k_w^A + k_X^A X + \sum_{i \neq X} k_{Qi}^A \, Qi)A \qquad [26]$$

and X(t) will be eliminated by assuming

$$X(t) = X(0) + A(0) - A(t) \equiv (X_o + A_o) - A(t) \qquad [27]$$

Equation 27 is valid because B(t) is always negligible in a flow containing more than 1 torr of water vapour (cf. [24]). X_o, the initial ground state O_2 concentration, is essentially zero for the chemical generation process since there is close to 100% $O_2(a)$ at the liquid/gas interface in the generator (Ref. 8). Deviations from this condition will be investigated.

When [27] is used for X in [26] a completely uncoupled first-order differential equation for A(t) results. This may be integrated directly to give:

$$A(t) = \frac{A_o K_T}{(K_T + k_D A_o) \exp(K_T t) - k_D A_o} \qquad [28]$$

where:

$$k_D \equiv k_p - k_X^A \qquad [29]$$

$$K_T \equiv k_w^A + k_X^A (A_o + X_o) + \sum_{i \neq X} k_{Qi}^A \, Qi \qquad [30]$$

The superscript A on the rate constants will be omitted in subsequent discussion since all constants involving B have been eliminated.

4.1 Estimation of the Pooling Rate Constant

Although A has been written A(t) in [28], it is more generally the many-variable function $A(t, A_o, X_o, \{k_{Qi}, Qi\}, k_w, k_p)$. So for a fixed time (at a fixed region in space in the flow system: the measurement cavity), [28] can generate $O_2(a)$ concentration as a function of total oxygen, given a set of values for the rate constants and quenching species concentrations. In particular, the experimental curve of Fig. 2 can be matched with a theoretical curve using values for k_w, k_p, k_x, k_{H_2O} and P_{H_2O} (partial pressure of water vapour in the system).

An estimate of the flow time between generator and cavity is required. We made a direct measurement of this time using two detector/chopper/lock-in amplifier combinations. One detector viewed the liquid-gas interface in the generator, while the other was at the downstream measurement cavity. Their voltage outputs were recorded on a dual-pen chart recorder, whose paper was set to move at 40 in/min. On opening the chlorine flow, we recorded a time delay between the detector signals of 0.43 s, reproducible to within 0.06 s. We therefore take:

$$t = 0.43 \pm 0.06 \text{ s} \qquad [31]$$

For the oxygen and water vapour quenching rate constants k_x and k_{H_2O}, the average of the two most recently reported values (Refs. 33, 34 and 31, 32 respectively) has been used in each case:

$$k_x = (1.5 \pm 0.1)\ \text{E-18} \ ; \ k_{H_2O} = (4.8 \pm 0.8)\ \text{E-18} \qquad [32]$$

The wall deactivation constant k_w was found to vary considerably (Refs. 31-35) depending on the condition and material of the walls. A glass tube freshly rinsed with HF, and evacuated for several hours, may have k_w as low as 0.1 (Ref. 35), whereas others have reported values in the range 0.2-0.6 (Refs. 32, 8). Only at higher pressures (above 100 torr) does k_w become pressure dependent (Ref. 32) (diffusion limited). The wall deactivation constant has therefore been treated in this study as a variable parameter. Since during the chemical generation process the walls near the generator become coated with a fine solid deposit (NaOH, NaCℓ), a higher wall deactivation rate can be expected.

The generally accepted literature value for the pooling rate constant is that of Derwent and Thrush (Ref. 20), who gave $k_p = (2.0 \pm 0.5)E-17$. Recently, Fisk and Hays (Ref. 37) also reported a value of 2.0E-17 for k_p, and gave an estimated uncertainty of ± 30%. A value of 2.4E-17 has also been quoted (Ref. 53). However, two independent groups (Refs. 21, 36) had previously obtained values about ten times lower than this (0.22, 0.23E-17, respectively). The first of these groups (Arnold and Ogryzlo) had also estimated an upper limit of 1.0E-17.

In this study, fixed values of k_p between 0.2E-17 and 3.0E-17 were investigated. For each value of k_p, eq. 28 was used to generate a numerical least-squares fit to points on the experimental curve of Fig. 2 by variation of the constant k_w. Twelve points were chosen at 0.5 torr intervals in the total O_2 pressure range 0.5 to 6 torr. Thus, for a given k_p an optimum curve can be obtained by numerical minimization (wrt k_w) of the least-squares function:

$$S \equiv \sum_{i=1}^{12} [(PO_2(a))_i^{expt.} - (PO_2(a))_i^{theory}]^2 \qquad [37]$$

A minor problem arises when eq. 28 is used with the experimental total O_2 pressures of Fig. 2. These were pressures at the measurement cavity, whereas the pressures in the generator/flow system up to the cavity were consistently 6% higher because there was a short (10 cm) length of smaller diameter tubing (2.5 cm) connecting the two regions. The effect of this small pressure difference has been included in the FORTRAN program that performs the numerical least-squares fits.

The form of the minimized S is shown in Fig. 3 over the range of values of k_p. There is a well-defined minimum at

$$k_p = 2.23E\text{-}17 \qquad [38]$$

for which the optimum wall deactivation rate constant is

$$k_w = 2.55 \qquad [39]$$

This pair of values (k_p, k_w) therefore gives the best possible fit to the experimental curve of Fig. 2.

Figure 4 shows our best-fit curve through the experimental points taken from the curve of Fig. 2. It also shows the best fit obtained using the k_p given by Arnold & Ogryzlo. It is evident that their value of 0.22E-17 for k_p cannot reproduce the curvature that we obtained experimentally.

4.2 Analysis of Errors in the Estimation of k_p

The value of k_p that minimizes S (eq. 37) depends on the values assigned to the following parameters:

1) the set of oxygen singlet delta concentrations at the measurement cavity; i.e. the experimental values $\{PO_2(a)\}$ of Figs. 2 and 4;

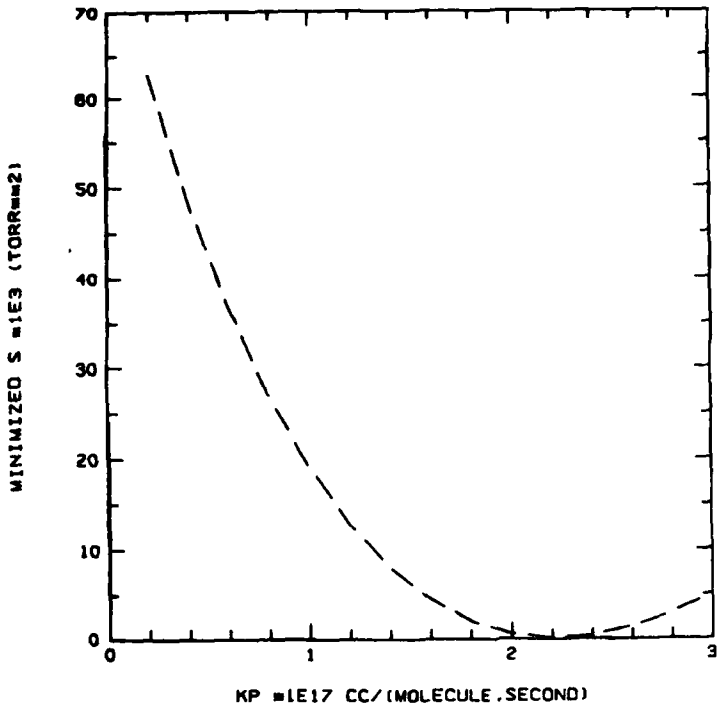

FIGURE 3 - Variation of minimized s with k_p

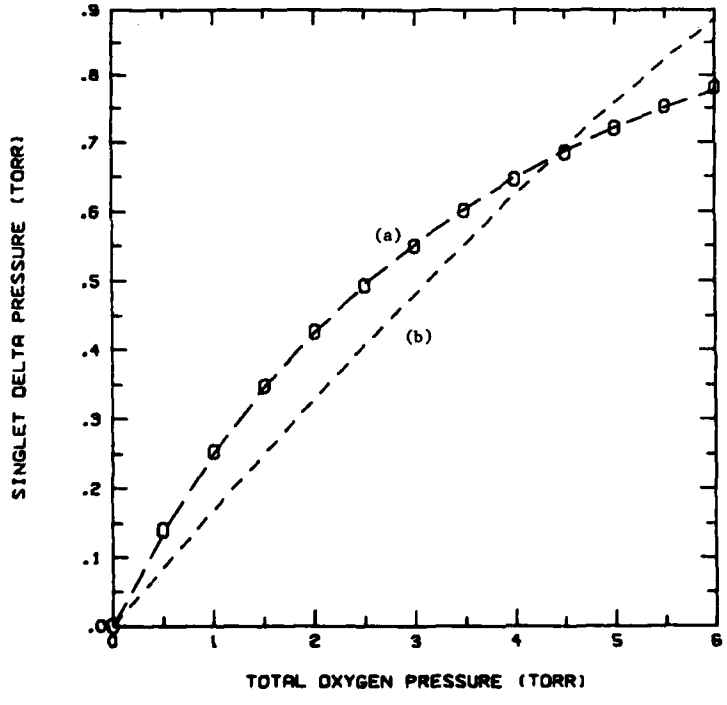

FIGURE 4 - Best-fit curves and experimental points

(a) This work: k_p = 2.23 E-17

(b) Arnold and Ogryzlo: k_p = 0.22 E-17

2) the amount of oxygen that is in the ground state at the generator solution/gas interface; i.e. X_o of eqs. 27 to 30;

3) the oxygen quenching rate constant k_x; and

4) the time t that molecules spend in the flow system from generator solution to measurement cavity.

The other parameters required in eqs. 28 to 30, which are quenching species concentrations and rate constants, only contribute to the pseudo-first-order rate constant K_T. They do not influence the computed value of the second-order constant k_p. However, they do affect the optimized value of k_w, which is therefore less accurately known than k_p. In this study, only H_2O vapour has been included as a quencher. The optimized values for k_w therefore contain contributions from pseudo-first-order quenching by H_2O_2 and $C\ell_2$. Since these have low concentrations in the gas stream, the contributions are expected to be small. First-order quenching due to solution droplets entrained in the gas stream also contributes to our value of k_w.

Table II shows the effect of the uncertainties in the input parameters on the optimized values for k_p and k_w (Δk_p, Δk_w) when a given parameter (column 1) takes either the maximum (+) or minimum (-) value defined by the error limits given in column 3. Thus, row 1 shows that when the experimentally measured $O_2(a)$ concentrations are decreased by 30% the best-fit k_p value increases by 0.0296E-17, a change of only 13%. The optimized k_w, on the other hand, increases by 33%. k_w is much more sensitive to changes in the absolute concentrations of $O_2(a)$ than is k_p. It is the curvature of $PO_2(a)$ as a function of increasing total oxygen pressure that is a sensitive measure of k_p (cf. Fig. 4). Row 2 indicates the effect of a deviation from 100% production of $O_2(a)$ at the generator. Initially, X_o was taken to be zero. When 10% of the total O_2 at the generator is taken to be in the

TABLE II

Effect of input parameter uncertainties on k_p and k_w

Parameter	Value	Uncertainty	$\Delta k_p \times 10^{17}$		Δk_w	
			(+)	(-)	(+)	(-)
$\{PO_2(a)\}$	Fig. 4	± 30%	-0.206	0.296	-0.612	0.833
X_o	0	+ 10% O_2	0.137	--	-0.246	--
k_x	1.5E-18	±0.1E-18	-0.025	0.025	0.005	-0.005
t	0.43	± 0.06	-0.319	0.422	-0.333	0.441
k_{H_2O}	4.8E-18	±0.8E-18	--	--	-0.039	0.039
$[H_2O]$	1.5 torr	±0.3 torr	--	--	-0.048	0.048

ground state, k_p increases by 6%, and k_w by 10%. It has been estimated (Ref. 8) that at least 95% of the oxygen is in the a-state at the generator, so that row 2 gives a generous estimate of this source of error.

Error limits for k_p and k_w can be established by combining the effects of the uncertainties in the parameters of Table II. We obtain:

$$k_p = 2.2 \text{ (+ 0.9 or -0.5) E-17} \qquad [40]$$

$$k_w = 2.6 \pm 1.3 \qquad [41]$$

The temperature of the gas also has an effect. The generator solution is in the -10 to -5°C range, and the gas arrives at the cavity at room temperature (20°C). However, recent publications (Refs. 51, 52) show the variation of k_p to be small from -15 to 20°C. If we assume the average gas temperature to be about 0°C, k_p would be reduced by approximately 10% from its value at 295 K.

Our results are therefore consistent with the recent values for k_p of about 2E-17 (Refs. 20, 37, 53).

5.0 CONCLUSIONS

Oxygen singlet delta can be chemically generated in a vacuum flow system without serious difficulty. Safe operating techniques and photometric methods for $O_2(a)$ concentration were developed for the generator that we constructed at DREV.

Operating at a pressure of 1 torr total oxygen, this generator produced (25 ± 7)% $O_2(a)$ at a downstream measurement cavity. The percentage $O_2(a)$ decreased to about 13% as the total O_2 pressure was increased to 6 torr. Argon and SF_6 used as diluent gases, up to a partial pressure of 10 torr, did not measurably alter this performance.

The excited oxygen is deactivated principally by water vapour, wall collisions, and energy-pooling. It should be possible to obtain close to 50% $O_2(a)$ in a downstream cavity by:

1) maintaining the generator solution temperature at -15°C;
2) minimizing the flow-system volume; and
3) doubling the pumping rate to about 20 L/s.

We estimate the pooling rate constant for oxygen singlet delta to be:

$$k_p = 2.2E\text{-}17 \text{ cm}^3 \text{ molecule}^{-1} \text{ s}^{-1} \qquad [43]$$

with upper and lower limits of 3.1E-17 and 1.7E-17 respectively. For the chemical generation process, a pseudo-first-order decay rate constant

$$k_w = 2.6 \pm 1.3 \text{ s}^{-1} \qquad [44]$$

is appropriate.

With these two values, eq. 28 may be used to predict the performance of any chemical oxygen generator if a reliable estimate of the generator to measurement cavity flow time is available.

This work on the chemical generation of oxygen singlet delta has given us the potential to rapidly develop a chemical oxygen iodine laser operating at 1.315 μm, and to study the blue-green emission at 529 nm arising from a pooling reaction between the singlet delta states of oxygen and nitrogen fluoride.

6.0 ACKNOWLEDGEMENTS

Ken Foster provided the ideas that initiated this project, and has since given us many useful suggestions. Georges Fournier, Leo Gingras and Maurice Lapointe have helped considerably with the construction and calibration of the semi-conductor detectors, while Maurice Verreault and Roger Lambert built the vacuum flow system. Maurice Verreault has also assisted in running every experiment, and has designed many improvements to the flow system.

7.0 REFERENCES

1. Wasseman, H.H. and Murray, R.W., "Singlet Oxygen", Academic Press, New York, 1979, Chapters 2 and 3.

2. McDermott, W.E., Pchelkin, N.R., Benard, D.J. and Bousek, R.R., "An Electronic Transition Chemical Laser", Appl. Phys. Lett., Vol. 32, p. 469, 1978.

3. Benard, D.J. and Pchelkin, N.R., "Measurement of $O_2(^1\Delta)$ Content in the Gaseous Effluents of a Chemical Generator", Rev. Sci. Instrum., Vol. 49, p. 794, 1978.

4. Benard, D.J., McDermott, W.E., Pchelkin, N.R., and Bousek, R.R., "Efficient Operation of a 100-W Transverse-flow Oxygen-Iodine Chemical Laser", Appl. Phys. Lett., Vol. 34, p. 40, 1979.

5. Richardson, R.J. and Wiswall, C.E., "Chemically Pumped Iodine Laser", Appl. Phys. Lett., Vol. 35, p. 138, 1979.

6. Richardson, R.J., Wiswall, C.E., Carr, P.A.G., Hovis, F.E. and Lilenfeld, H.V., "An Efficient Singlet Oxygen Generator for Chemically Pumped Iodine Lasers", J. Appl. Phys, Vol. 52, p. 4962, 1981.

7. Bachar, J. and Rosenwaks, S., "An Efficient, Small Scale Chemical Oxygen-Iodine Laser", Appl. Phys. Lett., Vol. 41, p. 16, 1982.

8. Laser Development for Laser Fusion Applications Research Progress Report, October 1979 - September 1980, SAND80-2823, Sandia National Laboratories, Albuquerque, New Mexico.

9. Busch, G.E., "Kinetic Analyses of Energy Storage in a Chemically Pumped Iodine Laser", IEEE J. Quant. Electronics, Vol. QE-17, p. 1128, 1981.

10. Derwent, R.G. and Thrush, B.A., "Excitation of Iodine by Singlet Molecular Oxygen", Farad. Discuss. Chem. Soc., Vol. 53, p. 162, 1972.

11. Badger, R.M., Wright, A.C. and Whitlock, R.F., "Absolute Intensities of the Discrete and Continuous Absorption Bands of Oxygen Gas at 1.26 and 1.065 μ, and the Radiative Lifetime of the $^1\Delta g$ State of Oxygen", J. Chem. Phys., Vol. 43, p. 4345, 1965.

12. Browne, R.J. and Ogryzlo, E.A., "Chemiluminescence from the Reaction of Chlorine with Aqueous Hydrogen Peroxide", Proc. Chem. Soc., p. 117, April, 1964.

13. Held, A.M., Halko, D.J. and Hurst, J.K., "Mechanisms of Chlorine Oxidation of Hydrogen Peroxide", J. Am. Chem. Soc., Vol. 100, p. 5732, 1978.

14. Chemical Safety Data Sheet SD-80, Manufacturing Chemists Association, Washington, D.C., 1960.

15. Data Sheet 207, National Safety Council, Chicago, 1966.

16. Chemical Safety Data Sheet SD-53, Manufacturing Chemists Association, Washington, D.C., 1961.

17. Schumb, W.C., Satterfield, C.N. and Wentworth, R.L., "Hydrogen Peroxide", Reinhold Publishing Corpn., New York, 1955.

18. Fisk, G.A. and Hays, G.N., "A Study of the 0.634 μm Dimol Emission from Excited Molecular Oxygen", Chem. Phys. Lett., Vol. 79, p. 331, 1981.

19. Falick, A.M. and Mahan, B.H., "Collisional-Radiative Reaction of $O_2(^1\Delta g)$", J. Chem. Phys., Vol. 47, p. 4778, 1967.

20. Derwent, R.G. and Thrush, B.A., "Measurements on $O_2\,^1\Delta g$ and $O_2\,^1\Sigma_g^+$ in Discharge Flow Systems", Trans. Far. Soc., Vol. 67, p. 2036, 1971.

21. Arnold, S.J. and Ogryzlo, E.A., " Some Reactions Forming $O_2(^1\Sigma_g^+)$ in the Upper Atmosphere", Can. J. Phys., Vol. 45, p. 2053, 1967.

22. Elias, L., Ogryzlo, E.A. and Schiff, H.I., "The Study of Electrically Discharged O_2 by means of an Isothermal Calorimetric Detector", Can. J. Chem., Vol. 37, p. 1680, 1959.

23. Findlay, F.D., "Relative Band Intensities in the Atmospheric and Infrared Atmospheric Systems of Molecular Oxygen", Can. J. Phys., Vol. 47, p. 687, 1969.

24. Whitlow, S.H. and Findlay, F.D., "Single and Double Electronic Transitions in Molecular Oxygen", Can. J. Chem., Vol. 45, p. 2087, 1967.

25. Findlay, F.D., "Visible Emission Bands of Molecular Oxygen", Can. J. Phys., Vol. 48, p. 2107, 1970.

26. Schurath, U., "The Energy Pooling Reaction $2O_2(^1\Delta g) \rightarrow O_2(^3\Sigma_g^-) + O_2(^1\Sigma_g^+)$; Formation, Relaxation, and Quenching of Vibrationally Excited $O_2(^1\Sigma_g^+)$", J. Photochem., Vol. 4, p. 215, 1975.

27. Borrell, P.M., Borrell, P. and Grant, K., "A Study of Three Dimol Emissions of Singlet Oxygen, $O_2(^1\Delta g)$, Using a Discharge Flow Shock Tube" J.C.S. Farad. II, Vol. 76, p. 1442, 1980.

28. Zhu, J.K., Li, J., and Pan, Y.K., "Radiative Lifetimes of the Singlet Oxygen Molecule", Chem. Phys. Lett., Vol. 78, p. 129, 1981.

29. Gray, E.W. and Ogryzlo, E.A., "The Cooperative Emission Bands of Singlet Molecular Oxygen", Chem. Phys. Lett., Vol. 3, p. 658, 1969.

30. Barton, S.A., "Estimation of the Concentration of a Photon-Emitting Gas in an Extended Source", DREV R-4290/83, March 1983, UNCLASSIFIED

31. Becker, K.H., Groth, W. and Schurath, U., "The Quenching of Metastable $O_2(^1\Delta g)$ and $O_2(^1\Sigma_g^+)$ Molecules", Chem. Phys. Lett., Vol. 8, p. 259, 1971.

32. Findlay, F.D. and Snelling, D.R., "Collisional Deactivation of $O_2(^1\Delta g)$", J. Chem. Phys., Vol. 55, p. 545, 1971.

33. Leiss, A., Schurath, U., Becker, K.H. and Fink, E.H., "Revised Quenching Rate Constants for Metastable Oxygen Molecules $O_2(a^1\Delta g)$", J. Photochem., Vol. 8, p. 211, 1978.

34. Borrell, P., Borrell, P.M. and Pedley, M.D., "Deactivation of Singlet Molecular Oxygen, $O_2(^1\Delta g)$, by Oxygen", Chem. Phys. Lett., Vol. 51, p. 300, 1977.

35. Clarke, I.D. and Wayne, R.P., "Collisional Quenching of $O_2(^1\Delta g)$", Proc. Roy. Soc. Lond. A, Vol. 314, p. 111, 1969.

36. Izod, T.P.J. and Wayne, R.P., "The Formation, Reaction and Deactivation of $O_2(^1\Sigma_g^+)$", Proc. Roy. Soc. Lond. A, Vol. 308, p. 81, 1968.

37. Fisk, G.A. and Hays, G.N., "Kinetic Rates in the Oxygen-Iodine System", J. Chem. Phys., Vol. 77, p. 4965, 1982.

38. Thomas, R.G.O. and Thrush, B.A., "Quenching of $O_2(^1\Sigma_g^+)$ by Ground State O_2", J.C.S. Farad. II, Vol. 71, p. 664, 1975.

39. Ogryzlo, E.A. and Thrush, B.A., "The Vibrational Excitation of H_2O and CO_2 by $O_2(^1\Sigma_g^+)$", Chem. Phys. Lett., Vol. 24, p. 314, 1974.

40. Davidson, J.A. and Ogryzlo, E.A., "The Quenching of $O_2(^1\Sigma_g^+)$ by Aliphatic Hydrocarbons", Can. J. Chem., Vol. 52, p. 240, 1974.

41. Davidson, J.A., Kear, K.E. and Abrahamson, E.W., "The Photosensitized Production and Physical Quenching of $O_2(^1\Sigma_g^+)$", J. Photochem., Vol. 1, p. 307, 1972.

42. Braithwaite, M., Ogryzlo, E.A., Davidson, J.A. and Schiff, H.I., "$O_2(^1\Sigma_g^+)$ Relaxation in Collisions. Part 2 - Temperature Dependence of the Relaxation by Hydrogen", J.C.S. Farad. II, Vol. 72, p. 2075, 1977.

43. Braithwaite, M., Ogryzlo, E.A., Davidson, J.A. and Schiff, H.I., "$O_2(^1\Sigma_g^+)$ Relaxation in Collisions. Temperature Dependence of the Interaction with HBr", Chem. Phys. Lett., Vol. 42, p. 158, 1976.

44. Braithwaite, M., Davidson, J.A. and Ogryzlo, E.A., "$O_2(^1\Sigma_g^+)$ Relaxation in Collisions. I. The Influence of Long Range Forces in the Quenching by Diatomic Molecules", J. Chem. Phys., Vol. 65, p. 771, 1976.

45. Stuhl, F. and Niki, H., "Kinetic Isotope Effects in the Quenching of $O_2(b^1\Sigma_g^+)$ by Some Deuterated Compounds", Chem. Phys. Lett., Vol. 7, p. 473, 1970.

46. O'Brian, R.J. and Myers, G.H., "Direct Flow Measurement of $O_2(b^1\Sigma_g^+)$ Quenching Rates", J. Chem. Phys., Vol. 53, p. 3832, 1970.

47. Lawton, S.A., Novick, S.E., Broida, H.P. and Phelps, A.V., "Quenching of Optically Pumped $O_2(b^1\Sigma_g^+)$ by Ground State O_2 Molecules", J. Chem. Phys., Vol. 66, p. 1381, 1977.

48. Martin, L.R., Cohen, R.B. and Schatz, J.F., "Quenching of Laser Induced Fluorescence of $O_2(b^1\Sigma_g^+)$ by O_2 and N_2", Chem. Phys. Lett., Vol. 41, p. 394, 1976.

49. Kear, K.E. and Abrahamson, E.W., "Electronic Energy Transfer in the Gas Phase: The Quenching of $O_2(^1\Sigma_g^+)$", J. Photochem., Vol. 3, p. 409, 1974.

50. Barton, S.A., "The General Chemical Kinetics Problem: A FORTRAN Program", DREV M-2543/81, April 1981, UNCLASSIFIED

51. Heidner, R.F., Gardner, C.E., El-Sayed, T.M., Segal, G.I. and Kasper, J.V.V., "Temperature Dependence of $O_2(^1\Delta) + O_2(^1\Delta)$ and $I(^2P_{\frac{1}{2}}) + O_2(^1\Delta)$ Energy Pooling", J. Chem. Phys., Vol. 74, p. 5618, 1981.

52. Borrell, P.M., Borrell, P., Grant, K.R. and Pedley, M.D., "Rate Constants for the Energy-Pooling and Quenching Reactions of Singlet Molecular Oxygen at High Temperatures", J. Phys. Chem., Vol. 86, p. 700, 1982.

53. Lilenfeld, H.V., Hovis, F.E., Richardson, R.J. and Ageno, H.Y., Tech. Digest Topical Meeting on Infrared Lasers, Los Angeles, California, December 3-5, 1980.

APPENDIX A

Transmission Factors

This section discusses the fraction of light, emitted in a band associated with some set of molecular transitions, that passes through a medium for which the transmittance is known as a function of wavelength.

Let $h(\lambda)$ be a function of wavelength describing the relative intensity of the light emitted in such a band, and let $h(\lambda)\delta\lambda$ be the fraction of all the photons in the band that are emitted in the infinitesimal wavelength interval $\delta\lambda$. Thus:

$$\int_0^\infty h(\lambda)d\lambda = 1 \qquad [A-1]$$

If $g(\lambda)$ gives the transmittance of the medium, then the fraction of photons from the band that passes through the medium in the interval $\delta\lambda$ is $g(\lambda)\ h(\lambda)\ \delta\lambda$.

A transmission factor, tf, may thus be defined for the entire band:

$$\int_0^\infty g(\lambda)\ h(\lambda)\ d\lambda \equiv tf \qquad [A-2]$$

An emission profile under low resolution may often be approximated by a Gaussian function, thus:

$$h(\lambda) = h_o \exp(\gamma(\lambda-\lambda_o)^2) \qquad [A-3]$$

and [A-1] may be used to define h_o, giving

$$h(\lambda) = (\gamma/\pi)^{\frac{1}{2}} \exp(-\gamma(\lambda-\lambda)^2) \qquad [A-4]$$

γ is given by the full width at half maximum (FWHM) of the emission peak:

$$\gamma = \frac{-4\ell n(0.5)}{(FWHM)^2} \qquad [A-5]$$

If the transmission medium is a window or a lens, for which the transmittance is generally a constant (T) over the wavelength region of the emission band, eq. A-2 is trivial:

$$(\ell tf) \text{ or } (wtf) = \int Th(\lambda)d\lambda = T \qquad [A-6]$$

The transmittance of a narrow-band interference filter, on the other hand, may often be approximated by a Gaussian:

$$g(\lambda) = \alpha \exp(-\beta(\lambda-\lambda_f)^2) \qquad [A-7]$$

where α is the maximum transmittance, at $\lambda = \lambda_f$, and β is calculated from the FWHM of the filter transmittance curve (cf. eq. A-5). Generally, the centre wavelength λ_f is chosen equal to λ_o for the emission band. In this case [A-2], [A-3] and [A-7] give:

$$(ftf) = \alpha(\gamma/\pi)^{\frac{1}{2}} \int_0^\infty e^{-(\gamma+\beta)(\lambda-\lambda_o)^2} d\lambda \qquad [A-8]$$

i.e.

$$(ftf) = \alpha(\gamma/\gamma+\beta)^{\frac{1}{2}} \qquad [A-9]$$

In general, the transmittance curve for the filter and the emission band profile may be treated pointwise in λ. The integral in [A-2] can then be calculated numerically to a high level of accuracy if many points are used.

In some cases the filter transmittance curve may be well approximated by a rectangle or a trapezium.

In the estimates of $O_2(a)$ concentrations described in this report, two emission bands were observed using different narrow-band interference filters.

(1) Dimole emission at λ_o = 634 nm

This was observed through a filter centred at 634.6 nm, with FWHM = 10.8 nm, and a transmittance curve well approximated by a trapezium (α = 0.61). The emission band is smooth with no resolved structure, FWHM = 15 nm (Refs. 24-26), and is well represented by a Gaussian form in the region of significant filter transmittance. The integral in [A-2] was performed numerically to yield:

$$(ftf)_{634} = 0.364 \pm 0.005 \qquad [A-10]$$

(2) Emission at λ_o = 1268 nm

A filter centred at 1268 nm, with FWHM = 20 nm and α = 0.54, was used. A Gaussian form approximated the transmittance curve. The emission band at low resolution (Refs. 23, 24) is also approximately Gaussian, with FWHM = 15 nm. Equation A-9 can then be used, with γ and β given by [A-5]:

$$(ftf)_{1268} = 0.43 \pm 0.01 \qquad [A-11]$$

DREV R-4310/83 (UNCLASSIFIED)

Research and Development Branch, DND, Canada.
DREV, P.O. Box 8800, Courcelette, Que. G0A 1R0

"Chemical Generation and Deactivation of Oxygen Singlet Delta" by
S. Barton

The construction and operation of a chemical generator of $O_2(a^1\Delta g)$ are described. This system could be readily modified to drive a purely chemical iodine laser operating at 1.315 μm.

Optical techniques were developed for estimating the excited oxygen concentration that arrives at a downstream cavity at total O_2 pressures from 1 to 6 torr.

Mechanisms that explain the deactivation of excited O_2 in the gas stream are discussed. A value for the singlet delta energy-pooling rate constant is determined from the measured $O_2(a^1\Delta g)$ concentrations.

DREV R-4310/83 (UNCLASSIFIED)

Research and Development Branch, DND, Canada.
DREV, P.O. Box 8800, Courcelette, Que. G0A 1R0

"Chemical Generation and Deactivation of Oxygen Singlet Delta" by
S. Barton

The construction and operation of a chemical generator of $O_2(a^1\Delta g)$ are described. This system could be readily modified to drive a purely chemical iodine laser operating at 1.315 μm.

Optical techniques were developed for estimating the excited oxygen concentration that arrives at a downstream cavity at total O_2 pressures from 1 to 6 torr.

Mechanisms that explain the deactivation of excited O_2 in the gas stream are discussed. A value for the singlet delta energy-pooling rate constant is determined from the measured $O_2(a^1\Delta g)$ concentrations.

DREV R-4310/83 (UNCLASSIFIED)

Research and Development Branch, DND, Canada.
DREV, P.O. Box 8800, Courcelette, Que. G0A 1R0

"Chemical Generation and Deactivation of Oxygen Singlet Delta" by
S. Barton

The construction and operation of a chemical generator of $O_2(a^1\Delta g)$ are described. This system could be readily modified to drive a purely chemical iodine laser operating at 1.315 μm.

Optical techniques were developed for estimating the excited oxygen concentration that arrives at a downstream cavity at total O_2 pressures from 1 to 6 torr.

Mechanisms that explain the deactivation of excited O_2 in the gas stream are discussed. A value for the singlet delta energy-pooling rate constant is determined from the measured $O_2(a^1\Delta g)$ concentrations.

DREV R-4310/83 (UNCLASSIFIED)

Research and Development Branch, DND, Canada.
DREV, P.O. Box 8800, Courcelette, Que. G0A 1R0

"Chemical Generation and Deactivation of Oxygen Singlet Delta" by
S. Barton

The construction and operation of a chemical generator of $O_2(a^1\Delta g)$ are described. This system could be readily modified to drive a purely chemical iodine laser operating at 1.315 μm.

Optical techniques were developed for estimating the excited oxygen concentration that arrives at a downstream cavity at total O_2 pressures from 1 to 6 torr.

Mechanisms that explain the deactivation of excited O_2 in the gas stream are discussed. A value for the singlet delta energy-pooling rate constant is determined from the measured $O_2(a^1\Delta g)$ concentrations.

CRDV R-4310/83 (NON CLASSIFIE)

Bureau - Recherche et Développement, MDN, Canada.
CRDV, C.P. 8800, Courcelette, Qué. GOA 1RO

"Génération chimique et désactivation de l'oxygène singulet delta" par S. Barton

On décrit la construction et le fonctionnement d'un générateur chimique d'oxygène $O_2(a^1\Delta g)$. Ce système pourrait être facilement modifié afin d'actionner un laser à iode entièrement chimique qui fonctionne à 1.315 μm.

On a développé des techniques optiques afin d'estimer la concentration de l'oxygène excité qui arrive dans une cavité située en aval du générateur. Des pressions totales d'oxygène de 1 à 6 torrs ont été étudiées.

On discute des mécanismes qui expliquent la désactivation de l'oxygène excité dans le flot de gaz. À partir des concentrations mesurées de $O_2(a^1\Delta g)$, on détermine une constante de vitesse de désactivation par un processus appelé mise en commun de l'énergie (energy-pooling).

CRDV R-4310/83 (NON CLASSIFIE)

Bureau - Recherche et Développement, MDN, Canada.
CRDV, C.P. 8800, Courcelette, Qué. GOA 1RO

"Génération chimique et désactivation de l'oxygène singulet delta" par S. Barton

On décrit la construction et le fonctionnement d'un générateur chimique d'oxygène $O_2(a^1\Delta g)$. Ce système pourrait être facilement modifié afin d'actionner un laser à iode entièrement chimique qui fonctionne à 1.315 μm.

On a développé des techniques optiques afin d'estimer la concentration de l'oxygène excité qui arrive dans une cavité située en aval du générateur. Des pressions totales d'oxygène de 1 à 6 torrs ont été étudiées.

On discute des mécanismes qui expliquent la désactivation de l'oxygène excité dans le flot de gaz. À partir des concentrations mesurées de $O_2(a^1\Delta g)$, on détermine une constante de vitesse de désactivation par un processus appelé mise en commun de l'énergie (energy-pooling).

CRDV R-4310/83 (NON CLASSIFIE)

Bureau - Recherche et Développement, MDN, Canada.
CRDV, C.P. 8800, Courcelette, Qué. GOA 1RO

"Génération chimique et désactivation de l'oxygène singulet delta" par S. Barton

On décrit la construction et le fonctionnement d'un générateur chimique d'oxygène $O_2(a^1\Delta g)$. Ce système pourrait être facilement modifié afin d'actionner un laser à iode entièrement chimique qui fonctionne à 1.315 μm.

On a développé des techniques optiques afin d'estimer la concentration de l'oxygène excité qui arrive dans une cavité située en aval du générateur. Des pressions totales d'oxygène de 1 à 6 torrs ont été étudiées.

On discute des mécanismes qui expliquent la désactivation de l'oxygène excité dans le flot de gaz. À partir des concentrations mesurées de $O_2(a^1\Delta g)$, on détermine une constante de vitesse de désactivation par un processus appelé mise en commun de l'énergie (energy-pooling).

CRDV R-4310/83 (NON CLASSIFIE)

Bureau - Recherche et Développement, MDN, Canada.
CRDV, C.P. 8800, Courcelette, Qué. GOA 1RO

"Génération chimique et désactivation de l'oxygène singulet delta" par S. Barton

On décrit la construction et le fonctionnement d'un générateur chimique d'oxygène $O_2(a^1\Delta g)$. Ce système pourrait être facilement modifié afin d'actionner un laser à iode entièrement chimique qui fonctionne à 1.315 μm.

On a développé des techniques optiques afin d'estimer la concentration de l'oxygène excité qui arrive dans une cavité située en aval du générateur. Des pressions totales d'oxygène de 1 à 6 torrs ont été étudiées.

On discute des mécanismes qui expliquent la désactivation de l'oxygène excité dans le flot de gaz. À partir des concentrations mesurées de $O_2(a^1\Delta g)$, on détermine une constante de vitesse de désactivation par un processus appelé mise en commun de l'énergie (energy-pooling).